ARMY RESEARCH LABORATORY

Quantitative Light-Scattering Angular Correlations of Conglomerate Particles

by Paul Pellegrino, Gorden Videen, and Ronald G. Pinnick

ARL-TR-1395 August 1997

Abstract

Quantitative analyses were performed of the fluctuations in the light-scattering intensities associated with micrometer-size glycerol droplets containing spherical latex inclusions. Scattering intensities at two angles (the near-forward and near-backward directions) were measured as a function of time. We analyzed these signals using two techniques. We find that calculated autocorrelation time constants associated with these signals are not consistent with current models that are based on interference of light scattering from latex inclusions exhibiting Stokes-Einstein diffusion. The intensity fluctuations at different scattering angles display extended periods of both positive and negative correlations with characteristic time constants on the order of seconds. The time constants associated with the cross-correlations provide information on the physical parameters of the inclusions.

Contents

Figures

Tables

1. Introduction

Research in aerosol physics, environmental physics, and biophysics has encouraged investigations into the light-scattering characteristics of complex scattering systems. One such system of particular interest is a host droplet containing contaminants. Recent research has focused on both elastic [1–5] and inelastic scattering [6–10] from a host droplet containing small inclusions. Unlike homogeneous droplets, these systems display a fluctuation in the scattered intensity as a function of time.

The inverse problem of calculating the contaminant characteristics from the scattered signal is fundamentally important. One would expect the scattering of the contaminants to be completely masked by the host because of its large size relative to the contaminant. In fact, the presence of inclusions within the host does not significantly alter the average angular scattering pattern produced by the host [3]. However, we do find that contamination of the host is revealed by a large fluctuation in the scattered intensity with time [2,3]. Analysis of this time-varying intensity provides important information on the type and extent of the contaminants.

In our study, we perform two separate photon-correlation analyses: autocorrelation and cross-correlation on the scattered intensities. Previous correlation analyses on scattering data [1,3] have used the autocorrelation function, which has been a workhorse of the dynamic light-scattering field. We examine the applicability of this autocorrelation technique to our scattering system and find that it fails to explain our observations. We then proceed to reexamine the system using a cross-correlation technique. This work is an extension of a previous photon-correlation study [4] in which the cross-correlation technique was employed to obtain qualitative information about different types of particle systems. In the previous cross-correlation study, we analyzed and compared the experimental data with data obtained numerically from an aggregate system and from a model of a sphere containing a single eccentric inclusion (representing a droplet containing a single Brownian particle). We were able to determine the nature of the particulate contamination (either an external aggregate or an internal inclusion) from the nature of the cross-correlations. In our present cross-correlation study, we are interested in obtaining quantitative information about the particle system: i.e., determining the dimensions of inclusions present in the droplet.

2. Experiment

Figure 1 shows a diagram of the experimental apparatus. The source is a cw KrAr mixed gas laser emitting on the krypton line at $\lambda = 647.1$ nm. The laser power is approximately 150 mW with optical noise of approximately 0.5 percent. The laser beam is focused by a long-focal-length lens ($f = 1.0$ m) before entering the scattering cell.

The scattering cell contains the electrodynamic particle trap. The cell is a capped acrylic cylinder that reduces air currents in order to maintain better droplet stability. The cylinder is fitted with beam entrance and exit holes of approximately 1 cm. The cell is equipped with a humidity sensor, since the humidity of the air has a direct effect on the water content of the trapped glycerol/water microdroplet. To minimize evaporation, we hold the droplets for approximately 1 hour in the electrodynamic trap so that equilibrium with

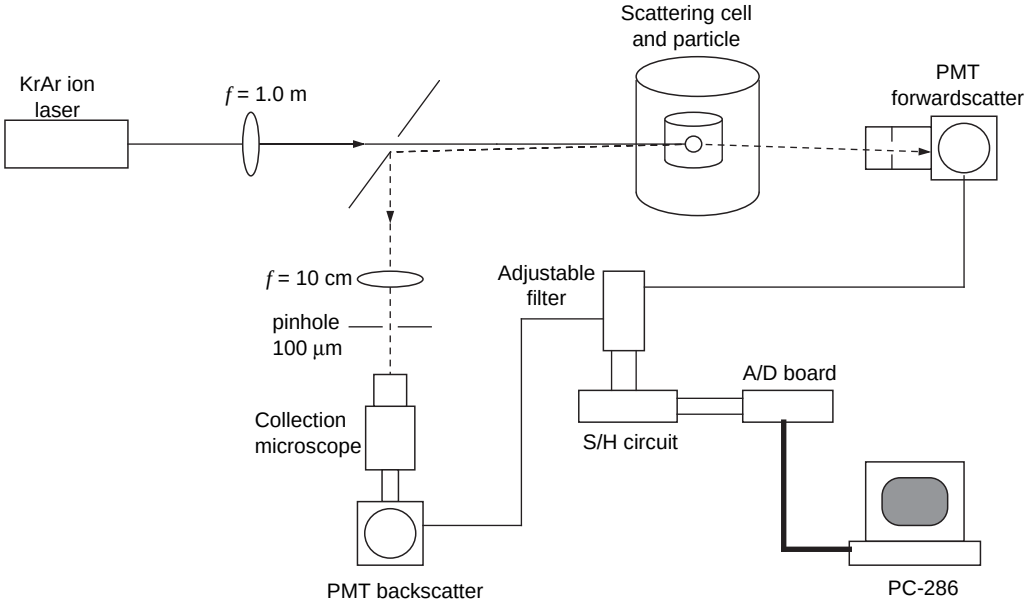

Figure 1. Schematic of experimental setup used to measure near-forward and near-backward elastic scattering from micrometer-size glycerol droplets seeded with latex particles. Droplets are caught in an electrodynamic trap and are illuminated with a KrAr laser ($\lambda = 647.1$ nm). Scattered light is simultaneously detected by PMTs placed in forward-scatter ($\sim 7°$) and backward-scatter ($\sim 179.5°$) directions. These signals are amplified, digitized, and stored.

the vapor within the scattering cell can be attained. However, since the cell is not completely airtight, some vapor does escape, and the host droplet slowly evaporates at a rate of approximately 0.2 nm over a 6-s data run.

The glycerol host droplet is located in the center of the electrodynamic trap. The trap enables a charged particle (glycerol droplet) to be held stationary by a combination of ac and dc fields. While the dc field offsets the gravitational force, the ac field works with the trap's geometry to create a quasi-stable area in the central region [11–13]. The glycerol droplets are created by a grounded atomizer, and these droplets are passed through a conducting ring held at high voltage (∼800 V). The ring can charge the droplet in two different ways: direct contact and differentially induced charging. Once charged, the droplets enter the trap through an entrance hole at the top. If the initial parameters (velocity, mass, and charge) of the droplet are within the stability curve of the trap (determined by ac and dc voltages, and trap dimensions), the droplet has a reasonable chance of being captured. This particular trap allows viewing in a plane perpendicular to the trap axis of symmetry from virtually any angle. We center the trapped droplet using the dc level and observe it with a microscope to ensure that it is completely stable.

The droplets are characterized by their diameter, water content, and contaminant concentration. The host glycerol droplets examined in this experiment have diameters in the range of $d_h \sim 20$ to 24 μm. We monitored and restricted the size of the host droplet to remove host size as a variable in the analysis. The knowledge of the host size provides an estimate of the number of inclusions. We determined the diameter of the host droplets by recording the angular intensity pattern for the first 10° using the forward-scatter photomultiplier tube (PMT) mounted on a rotation arm. These angular scattering data compared to a modified Fraunhoffer theory provide a determination of the host diameter to within 5 percent [14].

The water content is introduced into the solution via particle suspension. A previous study [15] of the evaporative dynamics of a levitated glycerol/water droplet concluded that the droplet loses most of its water content to the surrounding air almost immediately (∼10 min). A small percentage of water remains in the droplet. The residual amount of water depends on the relative humidity within the chamber, which generally remains between 20 and 30 ± 5 percent; this level of humidity results in a droplet water content of 5 to 10 percent by weight. Droplet water content determines the deviation of diffusion constant and index of refraction from that of bulk glycerol. The diffusion constant has a direct effect on the movement of the contaminants within the host droplet.

The contaminants, or inclusions, are uniform latex microspheres with diameters $d_i = 0.997 \pm 0.021$ μm (Duke Scientific Lot 5050A) and $d_i = 0.503 \pm 0.003$ μm (Duke Scientific Lot 3900A). These inclusion spheres are introduced into reagent grade glycerol, via a measured amount of particle suspension, as determined with a precision Mettler balance. Since the latex particle suspension specifications give concentrations to within ± 10 percent per milliliter, the mixture concentration of latex inclusions can be calculated to approximately the same uncertainty. We studied each latex-inclusion size at four separate concentration levels, made by diluting a base solution by factors of approximately 3. The large-diameter inclusions ($d_i = 0.997$ μm) have solution concentrations of approximately 1.9×10^{10}, 6.3×10^{9}, 2.1×10^{9}, and 6.9×10^{8} per millimeter. The small-diameter inclusions ($d_i = 0.503$ μm) have solution concentrations of approximately 2.5×10^{11}, 7.4×10^{10}, 2.7×10^{10}, and 9.3×10^{9} per millimeter. Each concentration analysis consists of data from several different host droplets (3 to 5 droplets).

The scattering signals from the trapped droplet are collected at the forward-scattering angle ($\sim 7^\circ$) by a Hamamatsu 1P28 PMT subtending a half-angle of approximately 0.12°. This small half-angle is achieved by a baffle-and-slit-configuration within the lighttight PMT housing. The backward scatter ($\sim 179.5^\circ$) is collected by a Hamamatsu R928 PMT, positioned 1.6 m away from the droplet. The scattered light reflects off a 45° angle mirror and passes through an imaging lens ($f = 10$ cm). The scattered light is then baffled via a pinhole ($d = 100$ μm) placed at the image plane, and finally arrives at the backward-scatter PMT via a collection microscope focused on the image plane. The backward-scatter PMT subtends a half-angle of approximately 0.12°. Both PMT signals are fed through a Rockland low-pass (250 Hz) filter and amplified. The filtered signals are captured simultaneously by two sample-and-hold (S/H) circuits toggled by a computer directly connected to the analog-to-digital converter (A/D), board. These devices hold the signals while the A/D picks off the values in succession. The overall sample rate (820 Hz), including the holding and collection, is dictated by the software interfacing and TTL (transistor-transistor logic) pulse signals needed to toggle the S/H circuit. This circuitry ensures simultaneous capture of the intensity signal. The acquisition time of the S/H circuit (AD582) to achieve 0.1 percent of a 10-V step is 6 μs. The signals are stored on a 286 PC interfaced to the A/D. In a typical run, 5000 data points are recorded over approximately 6 s. The A/D has 12-bit resolution with a signal range of ± 10 V, and an overall resolution of ± 2.44 mV. The shot noise is the dominant noise source, and is typically a small percentage of the signal.

3. Analysis

3.1 Autocorrelation Analysis

One of the main analysis tools employed by experimentalists investigating dynamic light scattering is the autocorrelation function [16,17],

$$\rho(t_j) = \frac{\sum_i (x_i - \bar{x})(x_{i+j} - \bar{x})}{\sum_i (x_i - \bar{x})^2} \ , \tag{1}$$

where $\overline{x}$ is the average intensity, x_i is the intensity at time t_i, and x_{i+j} is the intensity at time $t_i + t_j$, with $t_j = j \times \Delta t$. Light scattered by dynamic systems generally exhibits fluctuating signals. These fluctuating signals are often evaluated with an autocorrelation function in an attempt to quantify a time or length scale associated with the dynamic system. Previous research involving contaminated microdroplets analyzed the data using an autocorrelation function where the rate of decay is assumed to be [1]

$$\tau = \frac{1}{2q^2 D} \ , \tag{2}$$

and the propagation length vector

$$q = (4\pi/\lambda)\sin(\theta/2) \tag{3}$$

implicitly assumes interference as the source of the signal fluctuations. Equations (2) and (3) were derived for plane-wave illumination. The diffusibility is given by the Stokes-Einstein relation,

$$D = \frac{k_b T}{3\pi\eta d_i} \ , \tag{4}$$

where d_i is the diameter of the inclusion, k_b is Boltzmann's constant, T is the temperature, and η is the viscosity. By acquiring the time constant of the fluctuating signals, we can calculate the inclusion size:

$$d_i = \frac{8k_bTk^2}{3\pi\eta}\tau \ , \tag{5}$$

where $k = 2\pi/\lambda$ and measurements are made in the backscatter direction. Unfortunately, when this approach was applied [1] to the compound system of a host droplet containing spherical inclusions, the predictions were inconclusive due to a large spread in the time constants measured. In order to demonstrate the inadequacies of this analysis, we applied it to the large database of droplet information collected for this study. Table 1 shows the average time constants and the resulting calculated diameter compared to the actual diameter for both inclusion sizes at four different concentrations. The most noticeable feature in the average time constants is their large uncertainties. In addition, the sizes calculated for the loaded glycerol droplet by this technique are approximately an order of magnitude smaller than their actual sizes. The field striking the inclusions cannot adequately be described as a plane wave, and setting the propagation-length vector equivalent to $2k$ is questionable (as done in previous analyses [16,17]), but this value provides the largest estimated particle size that is still approximately an order of magnitude smaller than the specified diameter. Perhaps more importantly, the predicted sizes do not even scale linearly in τ, as suggested by the the-

Table 1. Results of autocorrelation analysis for glycerol host droplets containing uniform latex inclusions with diameters $d_i = 0.503$ and 0.997 μm.

Correlation time constants and inclusion sizes are presented for host droplets containing four different inclusion concentrations for each size. Calculation uses viscosity $\eta = 1.06$ kg m^{-1}s^{-1} at $T = 296$ K, which is an appropriate value considering water content of 5 to 10% by weight.

Concentration (No./ml)	Specified diameter (μm)	Average time constant, τ (s)	Calculated diameter (μm)
1.9×10^{10}	0.997 ± 0.021	0.25 ± 0.12	0.08 ± 0.04
6.3×10^{10}	0.997 ± 0.021	0.30 ± 0.21	0.09 ± 0.06
2.1×10^{9}	0.997 ± 0.021	0.30 ± 0.17	0.09 ± 0.05
6.9×10^{8}	0.997 ± 0.021	0.31 ± 0.19	0.10 ± 0.06
2.5×10^{11}	0.503 ± 0.003	0.19 ± 0.12	0.06 ± 0.04
7.4×10^{10}	0.503 ± 0.003	0.16 ± 0.09	0.05 ± 0.03
2.7×10^{10}	0.503 ± 0.003	0.20 ± 0.11	0.06 ± 0.03
9.3×10^{9}	0.503 ± 0.003	0.25 ± 0.17	0.08 ± 0.05

ory (eq (5)). The value of the average time constant for larger inclusions should be twice that of the smaller inclusions. Since the application of this technique on bulk solution containing particles is far more accurate than the application to contaminated droplets, we must conclude that this technique is insufficient to explain the dynamics of the droplet system decribed here.

3.2 Cross-Correlation Analysis

The complexity of the loaded-droplet system and the failure of the auto-correlation technique prompted a closer investigation of the light-scattering signals. The two-angle intensity measurements display some unusual features in terms of how the intensities behave in relation to one another. These features, along with a cross-correlation experiment conducted by Griffin and Pusey [18], suggest the application of the cross-correlation function to the two-angle intensity data. We consider data sets taken as a function of time, and explore the resulting correlations between them. For this, we use a standard correlation function defined as

$$\rho_{xy} = \frac{\sum_i (x_i - \bar{x})(y_i - \bar{y})}{\sqrt{\sum_i (x_i - \bar{x})^2 \sum_i (y_i - \bar{y})^2}} \ , \tag{6}$$

where x_i and y_i are the intensity signals measured at time t_i at two different scattering angles, and $\bar{x}$ and $\bar{y}$ are the time averages of these signals. The correlation function varies between $+1$ (the limit for perfectly correlated signals) and -1 (the limit for perfectly anticorrelated signals).

The analysis of the data records involves several steps. The data are first filtered by a 30-Hz median filter to remove shot noise. The filtered data are then processed by a Fortran program that calculates the cross-correlation. The cross-correlation for one time step is performed over an N-point ($N = 400$) window in the data set. This calculation is repeated across the entire data set to form the correlation as a function of time. Figure 2(a) shows an example of the filtered data, and figure 2(b) displays the corresponding cross-correlation. Several features are evident: a large negative correlation (~ -0.5) exists at the beginning half second of the data set, followed by a transition to an even larger positive correlation (~ 0.9), which trails off slowly over the final 1.5 s. This type of behavior, where a period of high correlation is followed by a period of high anticorrelation, or vice versa, is typical of other data we have taken. In order to gain better statistics for each host droplet, we measured between 8 and 20 data records and calculated the corresponding

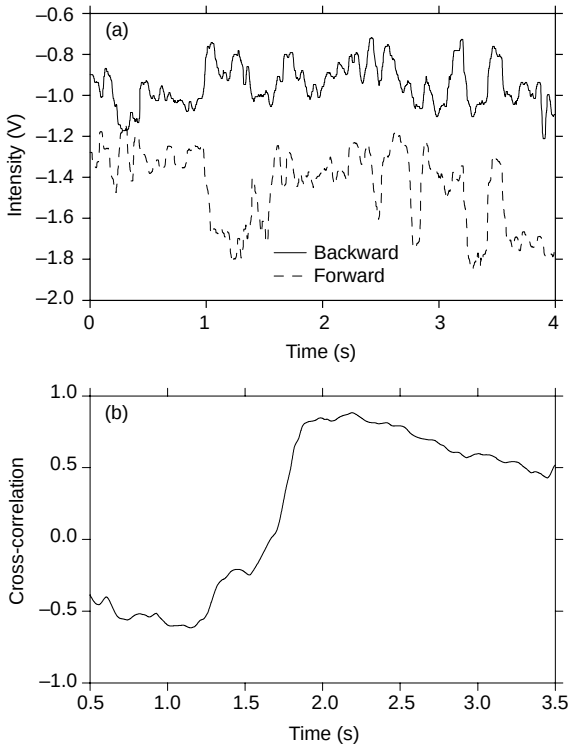

Figure 2. Forward-scatter and backward-scatter intensity of a host glycerol drop ($d_h \approx 24$ μm) containing approximately 15 ($d_i = 0.997$ μm) inclusions: (a) experimental data showing time variation and (b) correlation function of scattering signals.

cross-correlations. Although a cross-correlation as a function of time lag has been used in the past [18], the cross-correlation function plotted versus time provides qualitative information about how the system behaves. Therefore, we can view the cross-correlation function as an intermediate step in the data analysis process. We calculate the average of the squared correlation to further quantify the cross-correlations. This second moment provides information on the magnitude of the correlations. Figure 3 shows the average second moment for the correlations as a function of concentration. These curves indicate a slight decrease in correlation as the concentration increases. There is a difference in the second moments for the two inclusion sizes, but the large uncertainties make differentiation difficult.

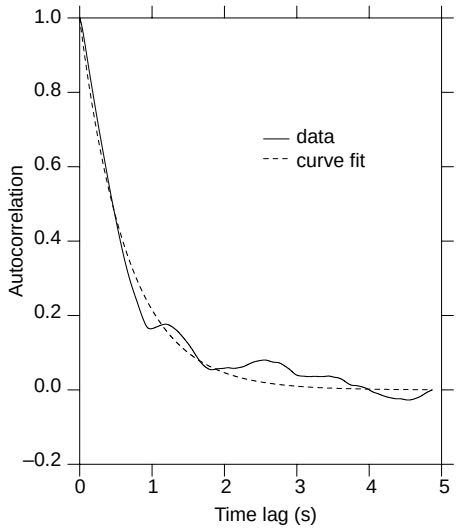

Figure 3. Average second moment of correlation between forward- and backward-scattering signals from host droplets containing inclusions as a function of concentration.

Another quantitative measure of the system requires an autocorrelation on the cross-correlation data for each data set. An examination of these autocorrelations provides a time constant associated with each grouping of cross-correlation data. The characteristic time associated with the decay of the correlations gives a different perspective on the light-scattering ensemble, and may be a key to understanding the physical process causing the correlations (and anticorrelations) of the scattering signals. The autocorrelation from each data run is summed, and the average of the set is fit to the function $y = e^{-t/\tau}$. A typical autocorrelation for a set of data is shown in figure 4, along with the fitted curve. An average time constant τ is determined by a least-squares analysis for each concentration that involves the data from several host droplets containing inclusions of the appropriate size. Figure 5 is a plot of the average time constants versus concentration for both particle sizes. The average time constants show virtually no dependence on inclusion concentration for either inclusion size, yet there is a distinct difference between the time constants for the different sizes. This analysis suggests that autocorrelation time constants associated with cross-correlations may be useful in determining the physical properties of contaminants contained within microdroplets.

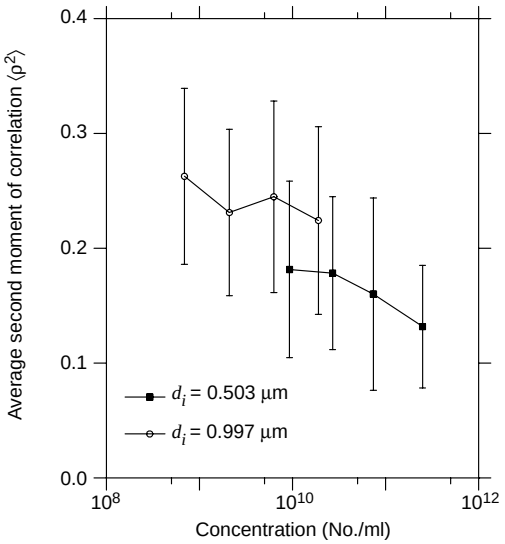

Figure 4. Example of autocorrelation performed on cross-correlation data set of $d_h \approx 21.6$ μm host sphere containing inclusions with diameter $d_i = 0.503$ μm and having concentration of 2.7×10^{10} per milliliter. Dotted line represents exponential fit of curve with time constant $\tau \approx 0.57$ s.

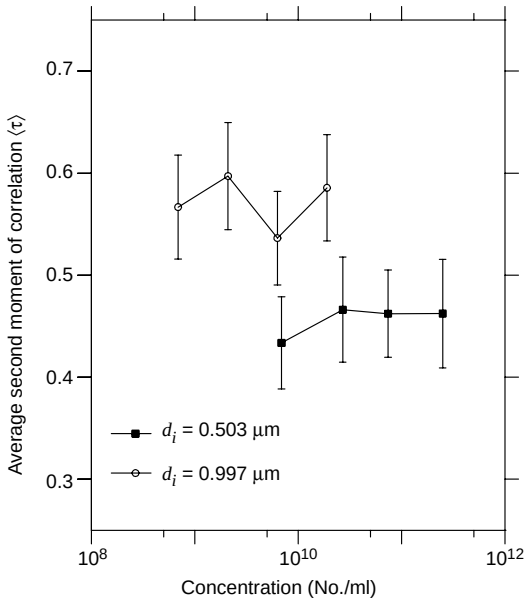

Figure 5. Average time constants associated with cross-correlation of forward- and backward-scattering signals for host glycerol droplets containing inclusions of two different sizes as a function of inclusion concentration.

4. Conclusion

The problem of quantifying a contaminated system from its scatter is generally difficult, since the scattering effects of a small inclusion in a large host are relatively small. In this study, two different techniques were used to examine the scatter from a host droplet containing uniformly sized inclusions. A standard autocorrelation particle-sizing technique predicted inclusion-size values well below the actual sizes, demonstrating the failure of this approach for determining the size of inclusions in a host. However, if correlations of the forward- and backward-scattering intensities are examined, time constants associated with these correlations appear to provide a means of determining the inclusion size, independent of the inclusion concentration.

Acknowledgments

Paul Pellegrino and Gorden Videen hold National Research Council research associateships at the Army Research Laboratory.

References

1. B. V. Bronk, M. J. Smith, and S. Arnold, "Photon-correlation spectroscopy for small spherical inclusions in a micrometer-sized electrodynamically levitated droplet," Opt. Lett. **18**, 93–95 (1993).

2. D. Ngo and R. G. Pinnick, "Suppression of scattering resonances in inhomogeneous microdroplets," J. Opt. Soc. Am. A **11**, 1352–1359 (1994).

3. J. Gu, T. E. Ruekgauer, J.-G. Xie, and R. L. Armstrong, "Effect of particulate seeding on microdroplet angular scattering," Opt. Lett. **18**, 1293–1295 (1993).

4. G. Videen, P. Pellegrino, D. Ngo, R. G. Pinnick, and P. Nachman, "Qualitative light scattering angular correlation of conglomerate particles," Appl. Opt. (in press).

5. G. Videen, P. Pellegrino, D. Ngo, R. G. Pinnick, and P. Nachman, "Light scattering angular correlation of spherical droplets containing inclusions," *Trends in Optics and Photonics Series* Vol. 2, *Advances in Optical Imaging and Photon Migration*, R. R. Alfano and James G. Fujimoto, eds. (Optical Society of America, Washington, DC, 1996), 45–49.

6. R. L. Armstrong, J.-G. Xie, T. E. Ruekgauer, and R. G. Pinnick, "Energy-transfer-assisted lasing from microdroplets seeded with fluorescent sol," Opt. Lett. **17**, 943–945 (1992).

7. H.-B. Lin, A. L. Huston, J. D. Eversole, A. J. Campillo, and P. Chýlek, "Internal scattering effects on microdroplet resonant emission structure," Opt. Lett. **17**, 970–972 (1992).

8. R. L. Armstrong, J.-G. Xie, T. E. Ruekgauer, J. Gu, and R. G. Pinnick, "Effects of submicrometer-sized particles on microdroplet lasing," Opt. Lett. **18**, 119–121 (1993).

9. J.-G. Xie, T. E. Ruekgauer, R. L. Armstrong, and R. G. Pinnick, "Suppression of stimulated Raman scattering from microdroplets by seeding with nanometer-sized latex particles," Opt. Lett. **18**, 340–342 (1993).

10. T. Kaiser, G. Roll, and G. Schweiger, "Enhancement of the Raman spectrum of optically levitated microspheres by seeded nanoparticles," J. Opt. Soc. Am. B **12**, 281–286 (1995).

11. E. James Davis and A. K. Ray, "Single aerosol particle size and mass measurements using an electrodynamic balance," J. Colloid Interface Sci. **25**, 566–576 (1980).

12. S. Arnold and L. M. Folan, "Fluorescence spectrometer for single electrodynamically levitated microparticles," Rev. Sci. Instrum. **57**, 2250–2253 (1986).

13. M. Essien, J. B. Gillespie, and R. L. Armstrong, "Observation of suppression of morphology-dependent resonances in singly levitated micrometer-sized droplets," Appl. Opt. **31**, 2148–2153 (1992).

14. T. W. Chen, "Simple formula for light scattering by large spherical dielectric, "Appl. Opt.**32**, 7568–7571 (1993).

15. E. James Davis, "Electrodynamic balance stability characteristics and applications to study aerocolloidal particles," Langmuir **1**, 379–387 (1985).

16. Cummins and Pike, *Photon Correlation Spectroscopy and Velocimetry* (Plenum Press, New York, 1977).

17. Robert Pecora, *Dynamic Light Scattering* (Plenum Press, New York, 1985).

18. W. G. Griffin and P. N. Pusey, "Anticorrelations in light scattering by nonspherical particles," Phys. Rev. Lett. **43,** 1100–1103 (1979).

Distribution

US Army Matl Cmnd
Dpty CG for RDE Hdqtrs
Attn AMCRD BG Beauchamp
5001 Eisenhower Ave
Alexandria VA 22333-0001

US Army Matl Cmnd
Prin Dpty for Acquisition Hdqrts
Attn AMCDCG-A D Adams
5001 Eieenhower Ave
Alexandria VA 22333-0001

US Army Matl Cmnd
Prin Dpty for Techlgy Hdqrts
Attn AMCDCG-T M Fisette
5001 Eisenhower Ave
Alexandria VA 22333-0001

US Army Mis & Spc Intllgnc Ctr
Attn AIAMS YDL
Redstone Arsenal AL 35898-5500

US Army NGIC
Attn Rsrch & Data Branch
220 7th Stret NE
Charlottesville VA 22901-5396

US Army Nuc & Cheml Agency
7150 Heller Loop Ste 101
Springfield VA 22150-3198

US Army Rsrch Lab
Attn SLCRO-D
PO Box 12211
Research Triangle Park NC 27709-2211

US Army Strtgc Defns Cmnd
Attn CSSD H MPL Techl Lib
Attn CSSD H XM Dr Davies
PO Box 1500
Huntsville AL 35807

US Military Academy
Dept of Mathematical Sci
Attn MAJ D Engen
West Point NY 10996

USAASA
Attn MOAS-AI W Parron
9325 Gunston Rd Ste N319
FT Belvoir VA 22060-5582

Chief of Nav OPS Dept of the Navy
Attn OP 03EG
Washington DC 20350

GPS Joint Prog Ofc Dir
Attn COL J Clay
2435 Vela Way Ste 1613
Los Angeles AFB CA 90245-5500

Ofc of the Dir Rsrch and Engrg
Attn R Menz
Pentagon Rm 3E1089
Washington DC 20301-3080

Special Assist to the Wing Cmndr
Attn 50SW/CCX CAPT P H Bernstein
300 O'Malley Ave Ste 20
Falcon AFB CO 80912-3020

USAF SMC/CED
Attn DMA/JPO M Ison
2435 Vela Way Ste 1613
Los Angeles AFB CA 90245-5500

ARL Electromag Group
Attn Campus Mail Code F0250 A Tucker
University of TX
Austin TX 78712

US Army Rsrch Lab
Attn AMSRL-CI-LL Tech Lib (3 copies)
Attn AMSRL-CS-AL-TA Mail & Records Mgmt
Attn AMSRL-CS-AL-TP Techl Pub (3 copies)
Attn AMSRL-IS-EE G Videen (15 copies)
Adelphi MD 20783-1197

REPORT DOCUMENTATION PAGE

Form Approved
OMB No. 0704-0188

1. AGENCY USE ONLY *(Leave blank)*	2. REPORT DATE	3. REPORT TYPE AND DATES COVERED
	August 1997	Progress, 1 Oct 1996 to 1 Oct 1997

4. TITLE AND SUBTITLE
Quantitative Light-Scattering Angular Correlations of Conglomerate Particles

5. FUNDING NUMBERS
PE: 61102A
DA: B53A

6. AUTHOR(S)
Paul Pellegrino, Gorden Videen, and Ronald G. Pinnick

7. PERFORMING ORGANIZATION NAME(S) AND ADDRESS(ES)
U.S. Army Research Laboratory
Attn: AMSRL-IS-EE
2800 Powder Mill Road
Adelphi, MD 20783-1197

8. PERFORMING ORGANIZATION REPORT NUMBER
ARL-TR-1395

9. SPONSORING/MONITORING AGENCY NAME(S) AND ADDRESS(ES)
U.S. Army Research Laboratory
2800 Powder Mill Road
Adelphi, MD 20783-1197

10. SPONSORING/MONITORING AGENCY REPORT NUMBER

11. SUPPLEMENTARY NOTES
AMS code: 611102.53A11
ARL PR: 7FEJ60

12a. DISTRIBUTION/AVAILABILITY STATEMENT
Approved for public release; distribution unlimited.

12b. DISTRIBUTION CODE

13. ABSTRACT *(Maximum 200 words)*

Quantitative analyses were performed of the fluctuations in the light-scattering intensities associated with micrometer-size glycerol droplets containing spherical latex inclusions. Scattering intensities at two angles (the near-forward and near-backward directions) were measured as a function of time. We analyzed these signals using two techniques. We find that calculated autocorrelation time constants associated with these signals are not consistent with current models that are based on interference of light scattering from latex inclusions exhibiting Stokes-Einstein diffusion. The intensity fluctuations at different scattering angles display extended periods of both positive and negative correlations with characteristic time constants on the order of seconds. The time constants associated with the cross-correlations provide information on the physical parameters of the inclusions.

14. SUBJECT TERMS	15. NUMBER OF PAGES
Contaminant, scatter	25
	16. PRICE CODE

17. SECURITY CLASSIFICATION OF REPORT	18. SECURITY CLASSIFICATION OF THIS PAGE	19. SECURITY CLASSIFICATION OF ABSTRACT	20. LIMITATION OF ABSTRACT
Unclassified	Unclassified	Unclassified	UL

NSN 7540-01-280-5500

Standard Form 298 (Rev. 2-89)
Prescribed by ANSI Std. Z39-18
298-102